The Influence of Vinyl Activating Groups on β-Allyl Sulfone-Based Chain Transfer Agents for Tough Methacrylate Networks

Paul Gauss,[1,2] Samuel Clark Ligon-Auer,[1,2] Markus Griesser,[1,2] Christian Gorsche,[1,2] Helena Svajdlenkova,[4] Thomas Koch,[5] Norbert Moszner,[2,3] Robert Liska[1,2]

[1]Institute of Applied Synthetic Chemistry, TU Wien, Getreidemarkt 9/163/MC, 1060 Vienna, Austria
[2]Christian Doppler Laboratory for Photopolymers in Digital and Restorative Dentistry, Getreidemarkt 9/163/MC, 1060 Vienna, Austria
[3]Ivoclar Vivadent AG, Bendererstrasse 2, 9494 Schaan, Liechtenstein
[4]Polymer Institute of the Slovakian Academy of Science, Dúbravská Cesta 9, 845 41 Bratislava, Slovakia
[5]Institute of Materials Science and Technology, TU Wien, Getreidemarkt 9, 1060 Vienna, Austria
Correspondence to: R. Liska (E-mail: robert.liska@tuwien.ac.at)

Received 27 September 2015; accepted 7 November 2015; published online 17 December 2015
DOI: 10.1002/pola.27993

ABSTRACT: In radical polymerization of monofunctional monomers, addition fragmentation chain transfer (AFCT) agents are well known to regulate polymerization and yield polymers with lower molecular weights and narrower molecular weight distributions. Papers concerning bulk photopolymerization of monomer mixtures with AFCT agents are rarely found in literature. In this article, AFCT reagents based on β-allyl sulfones with different vinyl activating groups were synthesized and compared. The compounds were tested in mono- and difunctional monomer systems providing information about the influence on photoreactivity, molecular weight, as well as thermal and mechanical properties of the resultant polymers. Where more potent activating groups (-Ph, -CN) markedly influenced polymerization at lower concentrations, the AFCT reagent with an ester activating group reacted at a similar rate to the methacrylate monomer ($C_T \approx 1$) and provided the best overall performance. © 2015 Wiley Periodicals, Inc. J. Polym. Sci., Part A: Polym. Chem. **2016**, *54*, 1417–1427

KEYWORDS: addition-fragmentation chain transfer; mechanical properties; methacrylates; networks; photopolymerization; shrinkage stress

INTRODUCTION Although the photopolymerization of (meth)-acrylates has been known for more than six decades, this technique is still finding more and more fields of advanced application in packaging, 3D-printing, coatings, and biomedical fields.[1,2] Important benefits of photo curing over thermal methods are that the reaction tends to be quicker and requires less energy. In addition, low molecular weight monomers are normally used to lower viscosity for processing, making the technology potentially free of volatile organic compounds.[3] While acrylates are more reactive and thus of greater interest in most industrial fields, methacrylate monomers are much less irritating to human skin and are thus preferred for dental and emerging tissue engineering applications.[4,5] Within these fields, shrinkage and associated shrinkage stress and high brittleness of the photopolymer networks remain as persistent problems.[6,7] A number of approaches have been taken to reduce shrinkage and shrinkage stress including the use of methacrylate monomers, which shrink less such as bisphenol-A glycidyl methacrylate and oligomeric methacrylates. Ring opening monomers are also investigated although poor reactivity has prevented their more widespread application.[8]

Chain transfer is yet another approach for modifying the cure kinetics and network architecture of a methacrylate-based polymer. Alkyl thiols are certainly one of the better studied classes of chain transfer agents, finding industrial application for the regulation of radical chain growth.[9] In the presence of thiols and a radical initiator, acrylates can undergo both propagation and chain transfer.[10] The propagation occurs to a greater extent so that a stoichiometric mixture of thiols and acrylates will still contain a substantial concentration of unreacted thiol after polymerization.[11] The reaction of alkyl thiols with methacrylates is by comparison substantially slower, which can also limit its utility. While thiols can be quite effective in improving the impact strength of acrylate and methacrylate-based resins, the Young's modulus of such polymers is significantly reduced due to flexible thio-ether linkages.[12] Other problems with thiols are odor

Additional Supporting Information may be found in the online version of this article.

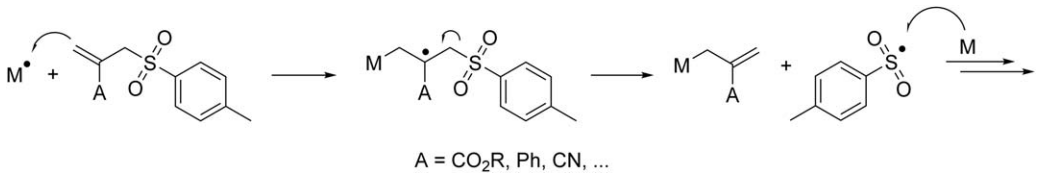

SCHEME 1 Mechanism of irreversible AFCT with β-allyl sulfone reagents.

and poor storage stability due to thermally induced Michael addition.[13] Where thiols function via transfer of a hydrogen atom, an alternate mode of chain transfer is that of addition-fragmentation chain transfer (AFCT).[14] AFCT may be classified as either reversible or irreversible. The first case, reversible AFCT (commonly shortened to RAFT) is a form of living polymerization and provides polymers with polydispersity index (PDI) values approaching unity.[15,16] More recently, photo-RAFT has been developed, however high conversions can take hours or days instead of seconds as is the usual case with (meth)acrylate polymerization.[17,18] Irreversible AFCT can also be used to regulate molecular weight. Although the PDI will not be as low as that achieved by RAFT (values of 1.5–2.0 are common),[19] polymerization can proceed at a rate comparable to that without chain transfer.

One of the more commonly used classes of irreversible AFCT agent (shortened throughout to CTA) is based on an α-olefin with a vinyl activating group and a labile bond near but not directly adjacent to the olefin.[14] The propagating radical will thus add to the CTA vinyl group and the resulting radical may then continue to propagate or fragment to form a new initiating radical. Although other relaxation paths are possible, the majority of CTAs are designed to fragment via β-scission. This gives rise to a terminal alkene and a new radical. The efficiency of chain transfer is then dependent on kinetics of addition and fragmentation, and on the initiation capacity of the newly formed radical. The labile bond of an irreversible CTA is normally a single bond between carbon and a heteroatom such as sulfur or phosphorus. In the first case, allyl sulfides are one of the better studied families of CTAs where the thiyl radical formed after fragmentation has good reactivity towards remaining vinyl monomers.[20] We have recently found that allyl sulfones are particularly efficient CTAs for regulating kinetic chain length in methacrylate-based networks (see mechanism depicted in Scheme 1).[21] Such β-allyl sulfone CTAs are effective reagents in dimethacrylate-based resins for lowering shrinkage stress and sharpening the glass transition of the network. More recently, difunctional β-allyl sulfone CTAs were found to improve impact strength while maintaining a high modulus.[22]

In this article, we investigate a series of β-allyl sulfone CTAs (see Fig. 1) with different vinyl activating groups. In comparison to the previously investigated ester 2-ethyl-2-(tosylmethyl)acrylate (**ASEE**), the other CTAs all have activating groups with different capability of stabilizing the intermediate radical, which should influence the rate of addition to the CTA and possibly allow better control of the network structure. Furthermore, the fairly high concentration of **ASEE** required to illicit an effect (typically 10–20 wt %) may limit its use in real world formulations.[23] Therefore, we concluded to also investigate the newly synthesized compounds at lower concentrations.

EXPERIMENTAL

Materials and Methods

All chemicals were purchased from Sigma Aldrich or Fluka and used as received unless otherwise noted. Dichloromethane (CH_2Cl_2) used for synthesis was of high purity grade. Urethane dimethacrylate (UDMA, CAS: 72869-86-4), 1,10-decandiol dimethacrylate (D_3MA, CAS: 72829-09-5) and bis(4-methoxybenzoyl)diethyl germanium (Ivocerin®)[24] were obtained from Ivoclar Vivadent and used as received. Bis(2,6-dimethoxybenzoyl)-2,4,4-trimethylpentylphosphine oxide (CGI403) was provided by Ciba. Melting points were measured on a Zeiss axioscope microscope with a Leitz heating block. GC-MS measurements were carried out on a Thermo Fisher Scientific DSQ II employing a Fused Silica capillary column (30 m × 0.25 mm). All experiments were performed at least in triplicate. Results are given as an average of three measurements with standard deviation.

Synthesis

2-Ethyl-2-(tosylmethyl)acrylate (ASEE)

Ethyl-2-(bromomethyl)acrylate (1 equiv, 4.83 g, 25 mmol), sodium *p*-toluenesulfinate (1.1 equiv, 4.9 g, 27.5 mmol) and polyethylene glycol 400 (0.025 equiv, 0.24 g, 0.6 mmol) were added to 35 mL THF. The resulting solution was refluxed for 3 h. Afterward, the mixture was extracted with 100 mL water and 3 × 100 mL diethyl ether. The organic phase was washed with brine (100 mL) and dried over Na_2SO_4. After

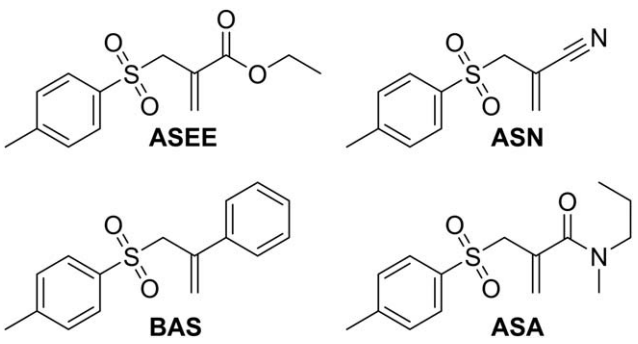

FIGURE 1 β-allyl sulfone CTAs with different activating groups.

evaporation of the solvent, the resulting oil was crystallized overnight. Recrystallization from diethyl ether yielded pure **ASEE** as colorless crystals (5.3 g, 79% yield).

Mp: 44.5 °C. TLC (R_f): 0.5 (PE/EtOAc=1:1). ^{1}H NMR (200 MHz, $CDCl_3$, δ, ppm): 7.72 (d, J = 8.22 Hz, 2H; Ar-H), 7.31 (d, J = 8.22 Hz, 2H; Ar-H), 6.50 (s, 1H; $=CH_2$), 5.91 (s, 1H; $=CH_2$), 4.14 (s, 2H; -SO_2-CH_2-), 4.01 (q, J = 7.24 Hz, 2H; -O-$C\underline{H}_2$-CH_3), 2.44 (s, 3H; Ar-CH_3), 1.18 (t, J = 7.04 Hz, 3H; -O-CH_2-$C\underline{H}_3$).

2-(Tosylmethyl)acrylonitrile (ASN)

Tosyliodide (4.88 g, 17 mmol) and methacrylonitrile (1.16 g, 17 mmol) were dissolved in CCl_4 (100 mL) and stirred at room temperature for 6 h. The solvent and any formed iodine were removed under vacuum. Another 100 mL CCl_4 was added along with triethylamine (TEA, 6.88 g, 68 mmol). The reaction was heated to reflux and after 12 h cooled to room temperature. The brown solution was then washed with a 5% solution of sodium dithionite (2 × 20 mL), 1N HCl (1 × 20 mL) and brine (1 × 20 mL). The organic phase was collected, dried with Na_2SO_4, filtered, and concentrated on a rotary evaporator. The product was further purified by column chromatography. About 790 mg 2-(tosylmethyl)acrylonitrile (**ASN**) was isolated as fine white needles (21% yield).

Mp: 109–110 °C. TLC (R_f): 0.5 (CH_2Cl_2). ^{1}H NMR (200 MHz, $CDCl_3$, δ, ppm): 7.73 (d, J = 8.45 Hz, 2H; Ar-H), 7.33 (d, J = 8.45 Hz, 2H; Ar-H), 6.15 (s, 1H; $=CH_2$), 5.94 (s, 1H; $=CH_2$), 3.84 (s, 2 H; -SO_2-CH_2-), 2.41 (s, 3H; Ar-CH_3).

2-(Tosylmethyl)styrene (BAS)

α-Methyl styrene (2.95 g, 25 mmol), tosyl chloride (4.77 g, 25 mmol), Cu(I)Cl (2.48 g, 25 mmol), and triethylamine (2.53 g, 25 mmol) were added to 70 mL dry acetonitrile and heated under argon to reflux. After 3 h, the reaction was cooled and diluted with 50 mL 0.1 N HCl. The mixture was extracted with CH_2Cl_2, the collected organic phases dried over Na_2SO_4, and the solvent was evaporated giving a brown crystalline raw product. Recrystallization from ethanol gave colorless crystals of poor purity. The product was further purified by column chromatography giving 3.60 g (53% yield) 2-(tosylmethyl)styrene (**BAS**) as a colorless solid.

Mp: 96–99 °C. TLC (R_f): 0.3 (CH_2Cl_2). ^{1}H NMR (200 MHz, $CDCl_3$, δ, ppm): 7.59 (d, J = 7.64 Hz, 2H; Ar-H), 7.5–6.9 (m, 7H; Ar-H), 5.51 (s, 1H; $=CH_2$), 5.14 (s, 1H; $=CH_2$), 4.18 (s, 2H; -SO_2-CH_2-), 2.32 (s, 3H; Ar-CH_3).

N-Methyl-N-propyl-2-(tosylmethyl)acrylamide (ASA)

(2-Bromomethyl)acrylic acid (8.25 g, 50 mmol) was dissolved in hot methanol (250 mL) and neutralized with NaOH (2 g, 50 mmol). Sodium *p*-toluenesulfinate (8.91 g, 50 mmol) was added in portions. The reaction mixture was then heated to reflux for 2 h and concentrated on the rotary evaporator. The concentrate was taken up with 500 mL water and acidified with 1 M HCl to give a precipitate. After cooling overnight the precipitate was filtered and washed with cold water (50 mL). Recrystallization from water gave 7.9 g (66% yield) of intermediate 2-(tosylmethyl)acrylic acid. Mp: 189–190 °C. ^{1}H NMR (200 MHz, $CDCl_3$, δ, ppm): 8.81 (bs, 1H, COOH), 7.67 (d, J = 8.6 Hz, 2H, Ar-H), 7.27 (d, J = 8.6 Hz, 2H; Ar-H), 6.55 (s, 1H; $=CH_2$), 5.94 (s, 1H; $=CH_2$), 4.04 (s, 2H; -SO_2-CH_2-), 2.36 (s, 3H; Ar-CH_3).

2-(Tosylmethyl) acrylic acid (3.00 g, 12.5 mmol) was refluxed in 30 mL thionyl chloride for 2 hours. Afterwards, excess thionyl chloride was removed by distillation under vacuum. The acid chloride was then dissolved in 100 mL anhydrous CH_2Cl_2 and cooled to 0 °C. To this solution *N*,*N*-methylpropylamine (75 mmol) was added dropwise. After 12 h at room temperature the solvent was removed. The crude product was dissolved in 50 mL CH_2Cl_2 and washed with 1 N HCl (2 × 20 mL) and brine (1 × 20 mL). After drying with Na_2SO_4, further purification of *N*-methyl-*N*-propyl-2-(tosylmethyl)acrylamide (**ASA**) was achieved by column chromatography. About 700 mg (19% yield) product was collected as a clear liquid.

TLC (R_f): 0.25 (PE/EtOAc 1:1 + 0.5% AcOH). ^{1}H NMR (200 MHz, $CDCl_3$, δ, ppm): 7.78 (d, J = 8.1 Hz, 2H; Ar-H), 7.34 (d, J = 8.1 Hz, 2H; Ar-H), 5.51 (bs, 1H; $=CH_2$), 5.41 (s, 1H; $=CH_2$), 4.09 (s, 2H; -SO_2-CH_2-), 3.5–2.7 (m, 5H; N-CH_3, N-$C\underline{H}_2$-CH_2-CH_3), 2.38 (s, 3H; Ar-CH_3), 1.7–1.3 (m, 2H; N-CH_2-$C\underline{H}_2$-CH_3), 0.85 (t, J = 7.5 Hz, 3H; N-CH_2-CH_2-$C\underline{H}_3$). ^{13}C NMR (50 MHz, $CDCl_3$, δ, ppm): 168.9 (C=O), 144.8 (C4), 136.5 (C4), 131.9 (C4), 129.8 (C3), 128.3 (C3), 124.24 (C2), 60.71 (C2), 50.5 (C2), 34.9 (C1), 21.6 (C1), 19.9 (C2), 11.1 (C1).

EIMS (70 eV) m/z (%): 295.05(2) $[M]^+$, 222.99(40) $[M\text{-}N(C_3H_7)(CH_3)]^+$, 154.99(60) $[TosSO_2]^+$, 140.09(100) $[M\text{-}TosSO_2]^+$, 91(48) $[C_6H_5(CH_3)]^+$.

Elementary analysis: Anal. Calcd. for $C_{15}H_{21}NO_3S$: C 60.99; H 7.17; N 4.74; S 10.85; found: C 60.18; H 7.30; N 4.76; S 10.74.

Sample Preparation for Analysis Monofunctional Test Systems

For the tests on the monofunctional system, benzyl methacrylate (BMA) with 1.0 wt % Ivocerin as photoinitiator was used as reference mixture. Samples were prepared with 5 double bond percent (db%) to 20 db% of CTA, depending on the solubility of the CTA. The db% refers to the percentage of all C=C double bonds in the system including monomer and CTA. To prepare each sample, monomer, the desired amount of CTA, and the photoinitiator were weighed into a brown glass vial, put into an ultra-sonic bath at 40 °C until the solids dissolved and then mixed with a vortex mixer.

Difunctional Test Systems

Samples for real-time (RT)-near-infrared (NIR) photorheology, dynamic mechanical thermal analysis (DMTA), and Dynstat impact resistance measurements were based on two dimethacrylate monomers (UDMA and D_3MA) as an equimolar mixture with 1.0 wt % Ivocerin as photoinitiator for the DMTA and Dynstat experiments and 0.3 wt % for the

rheology experiments. In both cases, samples were prepared with 5–20 db% of CTA, depending on the solubility of the CTA.

Photo-DSC

Photo-DSC was conducted on a Netzsch DSC 204 F1 with auto-sampler. The measurements were carried out at 25 °C under nitrogen atmosphere. Photoreactivity of the monomers was tested by weighing accurately 12 ± 0.5 mg of the sample into an aluminum DSC pan, which was subsequently placed in the DSC chamber after closing it with a glass lid. The sample chamber was purged with a N_2 flow (~ 20 mL min^{-1}) for 4 min and, subsequently, the samples were irradiated with filtered UV-light (400–500 nm) from an Exfo OmniCure S2000 broadband Hg-lamp with a light intensity of 1 W cm^{-2} at the exit of the light guide. The samples were exposed to light for 2 × 5 min, and the heat flow was recorded as a function of time. Time to attain 95% conversion ($t_{95\%}$) is defined as the time required for generated heat to equal 95% of ΔH_p.[25]

NMR Spectroscopic Analysis

NMR spectra (200 MHz for ^1H and 50 MHz for ^{13}C, respectively) were recorded with a Bruker AC 200 spectrometer. To determine the conversion of CTAs and BMA, the monomer mixtures and polymerized samples from photo-DSC measurements were dissolved in $CDCl_3$ (deuteration >99.5%). The solvent signal was used as internal reference. The conversion was calculated from the integral difference between the double bond peaks before and after curing. The signal of the tosyl methyl group from the CTAs appears as a singlet at about 2.6 ppm. This peak was used as reference, as it is not changed by polymerization. By normalizing the double bond signals of the CTA and of the monomer to this peak, it is possible to quantify the decrease of these signals after polymerization.

GPC

Following NMR, the samples were diluted with 0.5 mL THF and examined by GPC. GPC was performed with a Waters GPC using three columns connected in series (Styragel HR 0.5, Styragel HR 3 and a Styragel HR 4) and a Waters 2410 RI detector. The columns were maintained at 40 °C and a flow rate of 1.0 mL min^{-1} was used. Polystyrene standards were used for molecular weight calibration and THF was used as solvent. The polymers were not precipitated prior to GPC characterization.

Laser Flash Photolysis

Nanosecond transient absorption experiments were performed on a LKS80 Spectrometer (Applied Photophysics, UK). Excitation was performed using the third harmonic (355 nm, 10–20 mJ/pulse, ca. 8 ns) of a Spitlight Compact 100 (InnoLas, Germany) Nd:YAG laser. Concentration of CGI403 in acetonitrile was adjusted to achieve an absorbance of ca. 0.3 at 355 nm. The transient absorption spectra were recorded in a quartz cuvette (1 × 1 cm^2). Samples were purged and constantly bubbled with argon to refresh the sample and avoid sample decomposition. The rate constants for the addition of the phosphinoyl radicals to the monomer double bonds, k_{add}, were determined in pseudo-first-order according to the following equation $k_{obs} = k_0 + k_{add} \cdot k_{quencher}$.

RT-NIR Photorheology

RT-NIR photorheology experiments were performed on an Anton Paar MCR 302 WESP with a P-PTD 200/GL Peltier glass plate and a disposable PP25 measuring system. The rheometer is additionally coupled with a Bruker Vertex 80 FTIR spectrometer with external mirrors to guide the IR beam though the sample being analysed by rheology. In a typical experiment, 130 μL of sample was placed at the centre of the glass plate with the head of the rheometer held at a measuring position of 200 μm. The formulations were subjected to an oscillatory sheer with an angular strain of 1% and a frequency of 1 Hz. Polymerization was induced by UV-irradiation (300 s, 400–500 nm, 0.5 W cm^{-2}) projected via a waveguide from the underside of the glass plate using a filtered Exfo OmniCure S2000 broadband Hg-lamp. The IR beam also passes through the glass plate holding the sample and is reflected by the flat plate rheology head before returning to an external MCT detector. During the measurements, change in normal force along with the storage modulus and loss modulus were recorded. Data were collected with a frequency of 1 Hz before and 5 Hz during irradiation. The double bond conversion (DBC) was determined by recording a set of single spectra (time interval = 0.47 s) and then integrating the respective double bond bands at ~6160 cm^{-1}. The ratio of the double bond signal at the start and the end of the measurement were used to calculate the ultimate DBC. The final DBC is defined as the average DBC of the last 30 data points. DBC at the point of gelation (DBC_g) is defined as the conversion when the storage and loss modulus intersect. The time to 95% of total conversion t_{95DBC} is estimated graphically from the DBC diagram as the time till the moving average (5 measuring points) reaches 95% of total conversion. (c.f. Supporting Information).

Dynamic Mechanical Thermal Analysis

DMTA was performed with an Anton Paar MCR 301 with a CTD 450 oven and an SRF 12 measuring system. Rectangular (~ 5 × 2 × 40 mm^3) samples for DMTA were formed in a silicone mold placed into a Lumamat 100 light chamber (Ivoclar Vivadent), which provides light of 400–580 nm. Exposure was performed for 10 min on the top and 10 min on the back side. Samples were polished with sandpaper before placement into the DMTA. The samples were tested in torsion mode with a frequency of 1 Hz and strain of 0.1% and the temperature was increased from −100 to 200 °C with a heating rate of 2 °C min^{-1}. The glass transition temperature was defined as the temperature at the maximum dissipation factor (tan δ).

Dynstat Impact Resistance

Rectangular (~ 10 × 2 × 15 mm^3) samples for Dynstat tests were formed by curing in a silicone mold (details see DMTA). Samples were polished with sandpaper before

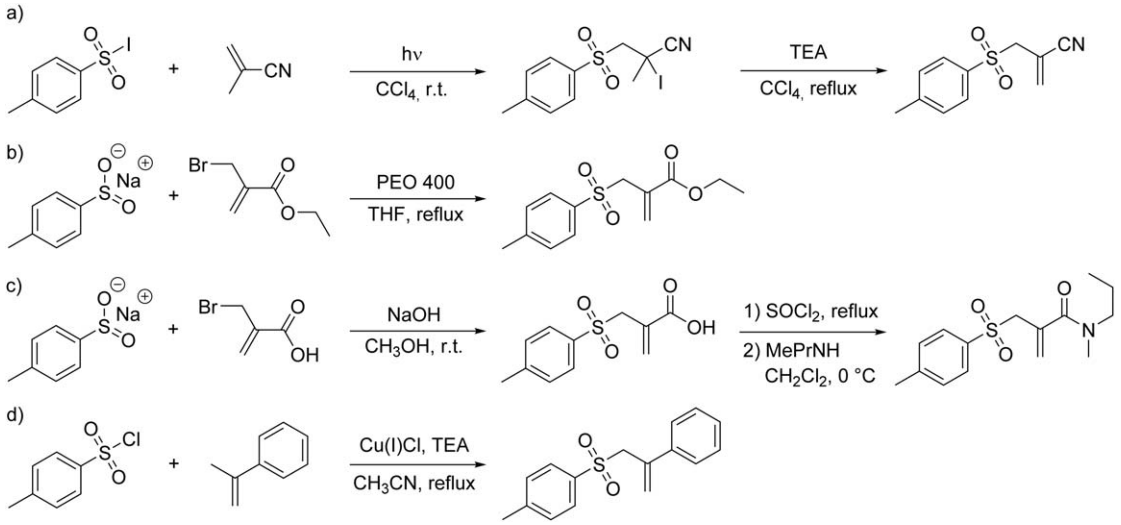

SCHEME 2 Synthetic routes to β-allyl sulfone CTAs.

placement into a Karl Frank Type 573 Dynstat machine. The samples were destroyed with a 5 kpcm hammer and the values were read from the scale. The results in kpcm were converted into kJ and divided by the area of fracture in m^2.

RESULTS AND DISCUSSION

Synthesis of β-Allyl Sulfone CTAs

Generally, β-allyl sulfones can be easily prepared by radical reaction of tosyl iodide with methacrylic acid derivatives.[26] The alkyl iodide intermediate addition product is then directly transformed (without workup) into the unsaturated sulfone by eliminating HI with TEA. This procedure was used for the synthesis of nitrile **ASN** in a yield of 21% [Scheme 2(a)] and can also be used for the synthesis of ester **ASEE**. Nevertheless, **ASEE** can be obtained more easily in high yield (79%) by condensation of ethyl 2-(bromomethyl)-acrylate with sodium *p*-toluenesulfinate [Scheme 2(b)].[27] Amide **ASA** could be synthesized by this method as well, but it was impossible to obtain the pure substance, as countless side reactions occurred during the process. Therefore, amide **ASA** was synthesized in two steps: (i) formation of 2-(tosylmethyl)-acrylic acid from 2-(bromomethyl)acrylic acid and sodium *p*-toluenesulfinate and (ii) reaction of the acyl chloride of the intermediate with *N*,*N*-methylpropylamine (13% overall yield) [Scheme 2(c)]. As the previously described general procedure did not lead to the desired product, two different synthetic routes to styrene-based **BAS** were tested. The first route was based on the addition of tosyl hydrazide to α-methylstyrene and provided the product in 41% yield.[28] By comparison, the copper catalyzed addition of *p*-tosyl chloride to methyl styrene followed by elimination with TEA provided **BAS** in 53% yield [Scheme 2(d)].[29]

None of the synthesized substances showed UV–vis absorption above 350 nm, so interference during polymerization using 400–500 nm light can be excluded.

Testing of CTAs in a Monofunctional Model Formulation

To better understand the reactivity of the synthesized CTAs, their copolymerization behavior and the influence on the molecular weight of formed polymers, photo-DSC, NMR, and GPC measurements were performed with a monofunctional methacrylate monomer (formulation **a**). Benzyl methacrylate (BMA) was used as monomer since the benzyl moiety does not interfere with the ^{1}H NMR signals of the CTAs. In addition BMA is a reasonable solvent for additives and is high boiling, which improves gravimetric analysis. Samples polymerized via photo-DSC could be used directly for NMR and GPC, such that the results of these three analytical methods should correlate directly for each sample.

Assessing the Photoreactivity of CTAs by Photo-DSC

Photo-DSC provides information on the kinetics and thermodynamics of the polymerization of BMA in the presence of different CTAs. In some cases, the solubility of the CTAs in the monomer was poor and limited the experiment to mixtures containing only 5 db% CTA (**ASN**, **BAS**). By comparison, ester **ASEE** and amide **ASA** were more soluble and could also be tested at higher concentrations. The time to reach the maximum rate of polymerization (t_{max}) is in the same range for all tested mixtures (Table 1). BMA is a monofunctional monomer which does not gel but does solidify when polymerized neat. Auto-acceleration is much less pronounced with BMA than with typical difunctional monomers and thus t_{max} is reached much later.[23] While CTAs moderate auto-acceleration of difunctional monomers and thus delay t_{max}, the effect is different with BMA. In this case, t_{max} is not delayed but actually comes slightly earlier. Also the time to reach 95% conversion ($t_{95\%}$) is reduced by addition of the tested CTAs. This indicates that the entire polymerization process (and not just the initial stages) is faster with CTAs. Explanation for both kinetic terms could be given by the fact that chain transfer should prevent runaway propagation and thus lower the viscosity of the reacting mixture. This should in turn allow monomers to diffuse more easily. Only mixture

TABLE 1 Analysis of BMA Polymerized Neat and with Different Concentrations of CTA (statistics c.f. Supporting Information)

			Photo-DSC			NMR		GPC	
Mixture	CTA	[CTA] (db%)	t_{max} (s)	$t_{95\%}$ (s)	DBC (%)	DBC – BMA (%)	DBC – CTA (%)	M_n (Da)	PDI
a	–	0	20.6	122	47	45	–	6,580	2.9
b	**ASEE**	5	19.0	107	43	45	56	1,530	2.3
c	**ASEE**	20	17.7	104	52	56	41	890	1.5
d	**ASA**	5	18.5	113	43	53	9.5	5,500	2.3
e	**ASA**	20	18.6	135	72	73	14	3,920	1.8
f	**ASN**	5	16.7	94.8	33	36	52	1,900	1.7
g	**BAS**	5	15.6	102	26	33	36	1,880	1.6

e containing 20 db% of amide **ASA** is slightly retarded compared to the pure monomer. This may be caused by steric hindrance of the CTA. From literature it is known that acrylamides are quite reactive, even more so than acrylic esters. Methacrylamides are by comparison much less reactive (a difference in reactivity even more dramatic than that between acrylic and methacrylic esters). Substitution on the N atom in methacrylamides further decreases the reactivity in homopolymerization dramatically. Disubstitution, even with methyl groups completely suppresses homopolymerization due to steric hindrance.[30]

Defining the transfer reaction as energy neutral,[21] which was recently proven for esters analogous to **ASEE**, heat measured in photo-DSC arises principally from the polymerization of BMA. The heat of polymerization was calculated from both NMR and DSC. To do so, pure samples of BMA were polymerized in the DSC device and the DBC of BMA in the samples was afterwards determined by NMR. Correlating the known conversion with the heat of polymerization measured in DSC gives the experimental ΔH_0 value for BMA ($\Delta H_0 = 52$ kJ mol^{-1}), which is close to 56 kJ mol^{-1} from literature.[31] Taking into account that the mixtures contain 80–95 mol % BMA, the measured heat of polymerization has to be corrected by the weight fraction of BMA (mass of BMA m_{BMA} divided by the total mass of the formulation m_{tot}). With eq 1, the DBC of BMA could be calculated from DSC.[21]

$$DBC_{DSC} = \frac{\Delta H}{\Delta H_0 \frac{m_{BMA}}{m_{tot}}} \quad (1)$$

Polymerization of BMA without CTA provided a DBC of ~ 45%. This rather low conversion is expected as BMA is not among the most reactive methacrylate monomers. As mixtures **b** and **c** show, ester **ASEE** has only marginal effects on the DBC of the monomer. On the other hand, mixture **e** containing 20 db% of amide **ASA** reaches a much higher DBC. Assuming that the transfer reaction is energy neutral, the less reactive and liquid amide could cause a thinning effect. Under these conditions, propagating radicals are less likely to recombine at low conversion and chains continue to grow for a longer time ($t_{95\%}$ is also much higher). This theory is supported by the fact that addition of 5 db% amide (**ASA**) shows no significant effect on the DBC in mixture **d** and has to be substantiated in the subsequent NMR experiments. The 5 db% mixtures of styrene-based **BAS** and nitrile **ASN** (mixtures **g** and **f**) show significantly reduced monomer DBC values. This can be rationalized by the good resonance stabilization of the generated radicals.

Conversion Determination by ^{1}H NMR Spectroscopy

To quantify the conversion of monomer and chain transfer reagent, ^{1}H NMR spectra of photo-DSC samples were recorded before and after irradiation. The difference in the integral of the vinyl protons directly correlates to the DBC of monomer BMA and of the CTA. As BMA and all of the CTAs have two vinyl protons, both signals were integrated and the arithmetic average was used for calculation of the DBC. In the case that vinyl proton signals of the CTA overlap with those of the monomer, only non-overlapping signals were integrated.

The center of Table 1 shows the conversion of neat BMA (mixture **a**) and of the CTA and BMA in all other formulations. The pure monomer BMA reaches a DBC of 45% as determined by NMR, which is very close to the value determined by DSC. Ester **ASEE** (mixtures **b** and **c**) and the monomer are consumed at comparable rates, so the molar ratio to BMA is nearly constant during the entire polymerization. This indicates a transfer constant C_T close to 1. On the other hand, DBC of amide **ASA** is very low at both tested concentrations (mixtures **d** and **e**). While DBC of the CTA is low, the conversion of BMA for the mixture with 20 db% **ASA** is much higher than all of the other samples. The low conversion of **ASA** supports the theory of a thinning effect proposed before. As the amide activated CTA is very unreactive, only small amounts take part in the polymerization while diluting the concentration of free radicals. Nitrile **ASN** (mixture **f**) is consumed at a much higher rate than the monomer, and therefore a $C_T > 1$ can be assumed. This seems reasonable, as this compound is highly activated by the nitrile moiety. In this set of experiments the styrene-based transfer agent **BAS** (mixture **g**) shows equal conversion as the monomer BMA, similar to **ASEE,** while reaching a much lower overall conversion. This indicates that the nitrile moiety of **ASN** is much more activating than the phenyl moiety of **BAS** and supports the hypothesis that propagation is slowed down by resonance stabilization of the aromatic ring.

When comparing the DBC results for BMA determined from DSC and from NMR, differences are in some cases observed. Although it is known that the transfer reaction can be assumed energy neutral for ester **ASEE**, the energy balance of the other CTAs may vary. In the case of mixture **g** with **BAS**, DBC of BMA as measured by DSC is significantly lower than the NMR value. This indicates some endothermic reactions. In no case, however, is DBC from photo-DSC greater and thus exothermic side reactions including propagation of CTA seem unlikely.

The Effects of CTAs on Molecular Weight, Established by GPC

Following NMR, GPC was performed on the BMA mixtures to determine the effect of the different CTAs on molecular weight. All of the CTAs lower the molecular weight and polydispersity of BMA (last two columns of Table 1). The effect is most pronounced in mixtures with ester **ASEE**, which was not surprising based on results from DSC and NMR. The number-average molecular weight M_n is drastically reduced from 6580 to 890 Da by addition of 20 db% of **ASEE** (mixture **c**). Moreover, the PDI decreases from 2.9 to 1.5, which indicates very good regulation and a homogenous incorporation of CTA. While the effect is more dramatic with 20 db% CTA, addition of 5 db% of **ASEE** (mixture **b**) also shows a strong regulating effect. By comparison, amide **ASA** (mixtures **d** and **e**) has a similar effect on PDI at both concentrations but molecular weight stays high. Considering the very low DBC of the CTA as measured by NMR, it looks like **ASA** does not transfer many chains during polymerization of BMA but rather reduces early stage chain termination by recombination. This still leads to a sharper molecular weight distribution, but is of little interest considering the low reactivity of the CTA. Nitrile **ASN** is very reactive and therefore, even in solutions with only 5 db% (mixture **f**), an effect is clearly visible. The molecular weight of BMA is strongly reduced to 1900 Da, while the PDI is lowered significantly as well. Also the reactive phenyl compound **BAS** shows a strong regulating effect. Only 5 db% reduces the molecular weight to 1880 Da while lowering the PDI to 1.6. While these results are indeed promising, the conversion of monomer in these mixtures only reached about 30%.

Determination of Addition Rates by LFP

To better understand the effect of different vinyl activating groups on the reactivity of β-allyl sulfones, laser flash photolysis (LFP) experiments were performed. As a model reaction, the addition rate constant (k_{add}) of an initiator radical to a CTA (or monomer) was determined. It should be noted that a different initiator (CGI403, bisacylphosphine oxide initiator) was used for LFP experiments. The reasons for this choice have been stated previously.[21] The reaction mixture was excited at 355 nm and the decay of the phosphinoyl radical absorption was followed at 450 nm.

Figure 2 shows the observed radical addition rates at varying concentration for the different CTAs and the two reference monomers benzyl and methyl methacrylate (MMA). The

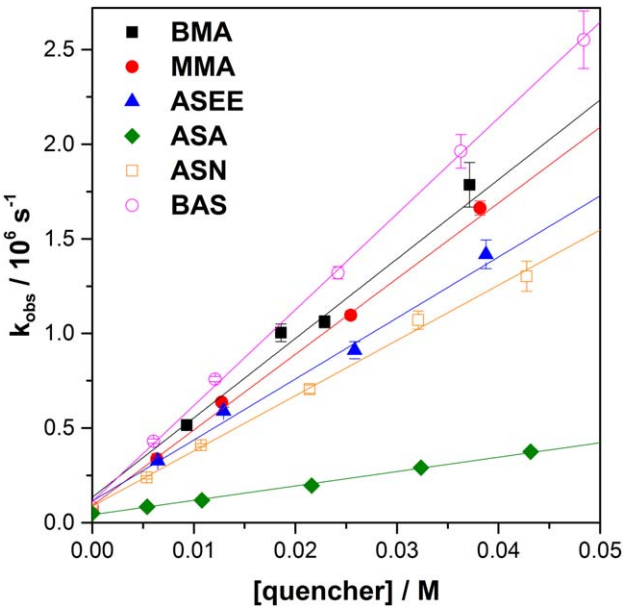

FIGURE 2 Observed addition rates versus concentration of monomers and CTAs. [Color figure can be viewed in the online issue, which is available at wileyonlinelibrary.com.]

determined k_{add} (pseudo first order) are collected in Table 2. It can be seen that for the better performing CTAs, the addition rate constant is comparable to that of methacrylates ($\sim 4 \times 10^7$ L mol^{-1} s^{-1}). Generally, all CTAs, except amide **ASA,** exhibit addition rate constants that are in a comparable range. Amide **ASA** shows a much lower k_{add} rate constant, which correlates well with the low CTA conversion values in photopolymerizations, determined by NMR experiments. The low addition rate is most likely caused by both sterical hindrance from the disubstituted amide group and subsequently weak radical stabilization because of the distorted geometry.[32] Styrene-based **BAS** shows the highest k_{add}, which is due mainly to the good resonance stabilization of the formed intermediate radical by the phenyl moiety. The high addition rate compared to methacrylates will lead to preferential addition to the CTA over the monomer. While addition is fast, the fragmentation reaction is likely to be the slowest among the tested CTAs, which explains the low conversion measured by NMR. It should be noted, that in the LFP experiment the attacking radical is a phosphinoyl moiety, which has a slightly different reactivity compared to the Germanium initiator radicals used in the other experiments, as well as polymer chain radicals. Nevertheless, the trends in reactivity determined from LFP likely hold true for the other experiments as well and are in general reflected in the conversion data.

It was not possible to determine significant differences for β-scission of the intermediate radicals as described previously.[21] Although the rate of β-scission is expected to be lowered when the intermediate CTA radical is highly resonance stabilized as in the case of nitrile **ASN** and phenyl modified **BAS**. Still, the β-scission reaction is preferred and

TABLE 2 Addition Rate Constants for Monomers and CTAs

Compound	k_{add} (10^7 L mol^{-1} s^{-1})
BMA	4.2 ± 0.1
MMA	4.0 ± 0.1
ASEE	3.2 ± 0.1
ASA	0.77 ± 0.05
ASN	2.9 ± 0.1
BAS	4.9 ± 0.1

addition of the intermediate radical to monomer was never observed.

Testing of Difunctional Monomers

A lot of industrial photocurable resins are based on dimethacrylate monomers. Cure kinetics and mechanical properties are important for virtually all applications. Therefore, after studying the β-allyl sulfones in mixtures with monofunctional BMA, they were tested with a dimethacrylate resin as well. As the resulting networks are insoluble, analysis by NMR and GPC is impractical. Instead, further information about the behavior of CTAs in difunctional monomer mixtures could be gathered by RT-NIR photorheology and DMTA. For photorheology measurements, the formulations consist of an equimolar mixture of commercially used dimethacrylates UDMA and D_3MA (mixture **A**), 0.3 wt % Ivocerin as photoinitiator and 5–20 db% of the β-allyl sulfone.

In Situ Investigation of Chemical and Rheological Behavior During Photocuring

The coupling of RT-NIR spectroscopy with photorheology is a very powerful tool for characterizing the curing reaction of a photopolymerizable formulation. Important metrics gathered from the technique include the time until gelation (t_g), conversion at the gel point (DBC_g), t_{95DBC}, final conversion (DBC), and shrinkage stress (normal force measurements, F_N).

In radical polymerization of dimethacrylates, crosslinking occurs already at fairly low conversion. After reaching the gel point, the polymer chains lack long-range mobility. As monomer conversion further increases, the material is exposed to high shrinkage stress as the gel cannot accommodate to the reduction of volume (see Fig. 3). By comparison, when gelation occurs at higher conversion, the system is flexible for longer and can rearrange to minimize stress. Following gelation, there will be less remaining monomer to contribute to the ultimate shrinkage stress. RT-NIR photorheology can be used to follow the process of gelation, by measuring t_g as the time where the storage modulus G' and loss modulus G″ plots intersect ($G''/G' = 1$). At this time point, the DBC_g can also be determined.

Gel Point

As can be seen in Table 3, gelation of the reference mixture **A** occurs after only 4.2 s, at which point a DBC_g of 22% is measured. In all AFCT moderated systems t_g generally occurs later than in the reference. More importantly, most samples

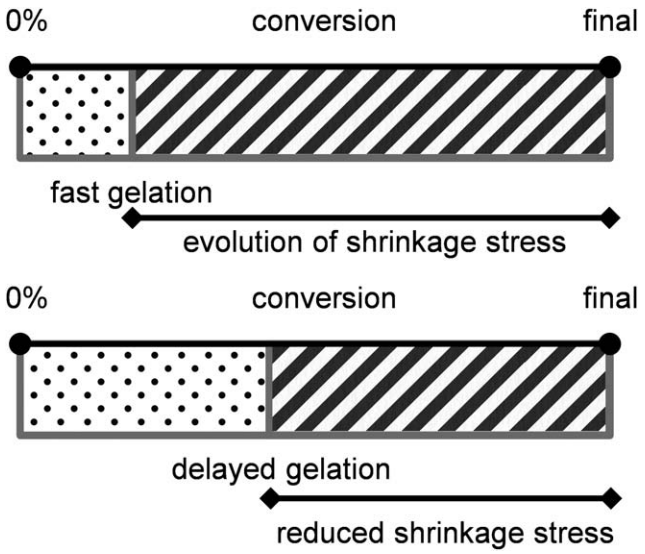

FIGURE 3 Higher conversion at the gel point results in reduced shrinkage stress (liquid = dotted, solid = dashed).

reach a higher DBC_g than the reference. Impressively, the DBC_g is increased to nearly 30% with the addition of 5 db% of ester **ASEE** (mixture **B**). Adding 20 db% of **ASEE** increases the DBC_g up to 41%. Mixtures **D** and **E** containing amide **ASA** show a slightly improved DBC_g, but nearly no delay of t_g is witnessed. These results are in good agreement with the monofunctional methacrylate experiments and once again attest to the low reactivity of amide **ASA**. By comparison, adding only a small amount of nitrile **ASN** (mixture **F**) causes an enormous delay of t_g while showing a lower DBC_g than the reference. Both metrics are indicative of poor polymerization performance. As initiator concentration and light intensity are low in this experiment, the retardation caused by the strongly resonance stabilized CTA is more pronounced. Styrene-based **BAS** shows better performance, as the t_g of mixture **G** is strongly delayed while the DBC_g is raised slightly.

TABLE 3 Results from RT-NIR-Photorheology with Commercial Monomers UDMA and D_3MA in Equimolar Ratio, Showing the Time to Gelation (t_g), the Double Bond Conversion at the Time of Gelation (DBC_g), the Overall Conversion (DBC), and the Shrinkage Stress as Maximal Normal Force (F_N) (statistics c.f. Supporting Information)

Network	CTA	[CTA] (db%)	t_g (s)	DBC_g (%)	t_{95DBC} (s)	DBC (%)	F_N (N)
A	–	0	4.2	22	87	73	−29.6
B	**ASEE**	5	9.9	29	108	74	−18.6
C	**ASEE**	20	36.5	41	184	75	−14.7
D	**ASA**	5	5.2	27	108	73	−14.0
E	**ASA**	20	6.1	29	119	74	−11.2
F	**ASN**	5	45.7	17	244	48	−13.1
G	**BAS**	5	38.6	30	227	57	−17.6

Time to 95% of Total Conversion

The time to reach 95% of total conversion (t_{95DBC}) is a good metric for retardation. It is clearly visible that all transfer agents cause some retardation. At 0.5 W cm^{-2} light intensity and with only 0.3 wt % of initiator, the retardation caused by the highly resonance stabilized nitrile **ASN** and styrene-based **BAS** is significant (factor $\approx$ 3).

Overall Double Bond Conversion

RT-NIR allows the tracking of DBC, by monitoring the decrease of the area of the double bond peak at $\sim$6160 cm^{-1} during the curing reaction. The reference sample without CTA reaches a final DBC around 73%. By comparison, the mixtures containing ester **ASEE** and amide **ASA** reach this value as well. On the other hand, the resonance stabilized CTAs based on nitrile (**ASN**) and styrene (**BAS**) cause a significant decrease in final conversion. From the basic investigations on BMA, this was well expected. In both cases, the formed intermediate radical is so well stabilized, that fragmentation happens significantly slower.

Shrinkage Stress

Monitoring of the force normal to the cure surface (F_N) during photorheometry gives an indication of shrinkage stress as it develops during polymerization. The measured F_N for the dimethacrylate reference mixture **A** was nearly 30 N. F_N for all of the other mixtures is greatly reduced. In prior investigations,[22] a good correlation between the DBC_g and the evolution of F_N has been found. Indeed mixtures with higher DBC_g values show lower F_N values (c.f. Table 3).

Interestingly, the amount of CTA needed to reduce the shrinkage stress seems to be rather low, as all mixtures with 5 db% CTA show good F_N values (**B**, **D**, **F**, and **G**). The mixture with 20 db% of unreactive amide **ASA** (mixture **E**) has the highest reduction in shrinkage stress. This result can be caused by a combination of chain transfer reaction and thinning of the monomer formulation causing a lower network density at the gel point. Formulations with 5 wt % of **ASN** and **BAS** have greatly reduced shrinkage stress, which is to be expected with these slower polymerizations reaching lower final monomer conversion. **ASEE** does a very good job of lowering shrinkage stress, and in mixture **C** with 20 db% the reduction is 50%.

DMTA

To investigate the glass transition of the dimethacrylate networks, DMTA measurements were performed. In these experiments, the storage modulus (G') and loss factor (tan δ) plots of the β-allyl sulfone modified dimethacrylate networks are tracked relative to the unmodified polymer. Regulation of polymerization with CTAs affects the glass transition temperature of the resultant network. In all cases, the glass transition was both lowered and sharpened, which is indicative of a more regular and homogenous network. The sharpness of the transition is quantified as the full width at half maximum (FWHM) of the tan δ peak (see Table 4).

TABLE 4 Results of DMTA Measurements with Commercial Monomers UDMA and D_3MA in Equimolar Ratio and Various CTAs

Network	CTA	[CTA] (db%)	$G'_{20°C}$ (MPa)	FWHM (°C)	T_g (°C)	G'_r (MPa)
A	-	0	1,060	144	144	813
B	**ASEE**	5	1,020	47	121	280
C	**ASEE**	20	1,070	28	48	45
D	**ASA**	5	953	126	133	637
E	**ASA**	20	888	58	66	191
F	**ASN**	5	982	93	126	470
G	**BAS**	5	1,090	82	124	390

Ester **ASEE** produced the most homogenous polymer networks with an extraordinary low and sharp glass transition. (Fig. 4) This is due to its radical addition rate being comparable to the methacrylate monomer, and the CTA is therefore built into the network statistically. While the other CTAs also lower and sharpen the glass transition, the effect is less pronounced. It is also important to note that the modulus at room temperature of the **ASEE** the modified polymers (mixtures **B** and **C**) is in the same range as the reference. By comparison, the amide **ASA** has a much weaker influence on the glass transition while consequently lowering modulus (mixtures **D** and **E**). As prior tests with **ASA** all showed poor reactivity and conversion, the reagent is likely doing little more than softening the network.

The formulations with 5 db% of **ASN** (**F**) and **BAS** (**G**) exhibit similar DMTA curves. The storage modulus and dissipation factor curves of both mixtures run congruent with each other, although the polymer formed from mixture **F** shows a much lower storage modulus at room temperature (Table 4). Both CTAs are more effective than **ASA** at 5 db% in sharpening and lowering the glass transition. As these reagents were found in previous measurements to be highly reactive, it is likely that most of the CTAs reacted at the beginning of the polymerization. Thus, very short chains were produced in early stages while the majority of monomer propagation was left unregulated. This is supported by the fact that there are at least two glass transitions overlaying each other in the tan δ diagram (c.f. Supporting Information) Furthermore, one has to keep in mind that DBC is significantly lower than in previously mentioned samples.

Unfortunately, it was not possible to measure samples with concentrations of **ASN** or **BAS** higher than 5 db% as they tended to crystallize during preparation.

Dynstat Impact Resistance

To determine the effect of chain transfer on impact resistance, Dynstat tests were performed with all of the cured polymer mixtures. The Dynstat tests clearly show that the impact resistance is improved in all cases with addition of CTA (Table 5). Ester **ASEE** causes the largest effect, and in polymer network **C** with 20 db% of this CTA impact

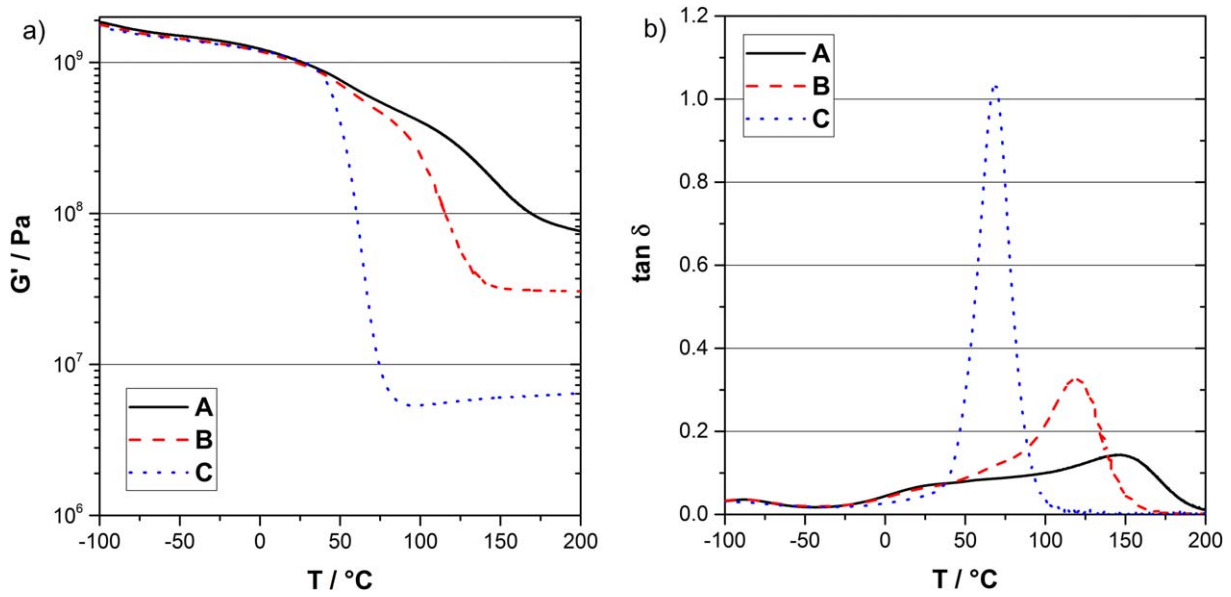

FIGURE 4 Storage modulus (G') and loss factor (tan δ) plots of reference network A, and ASEE containing formulations B and C. [Color figure can be viewed in the online issue, which is available at wileyonlinelibrary.com.]

resistance is increased by a factor of 2.5. Amide **ASA** is also capable of improving the toughness but the effect is smaller. Phenyl substituted **BAS** allows a rather significant improvement in impact resistance already at 5 db%. Nitrile **ASN**, by comparison, provides a polymer with impact resistance little different from the control.

From DMTA it was determined that the polymer containing 5 db% **ASN** had a slightly higher modulus than the reference, which indicates a hard but also brittle material. The polymer with 5 db% **BAS**, on the other hand, is less brittle but also less hard. Where high values of both modulus and impact strength are desired, the polymers with **ASEE** (**B** and **C**) are the most satisfactory.

CONCLUSIONS

In this article, we have presented β-allyl sulfones with different activating groups and assessed their influence on the polymerization behavior and final material properties of mono- and difunctional methacrylates.

The behavior of β-allyl sulfones is dramatically changed by variation of the vinyl activating moiety. Activating groups such as phenyl and nitrile, which offer good resonance stabilization for the intermediate CTA radical, significantly increase the rate of radical attack on the CTA. However, good resonance stabilization also slows down the β-scission fragmentation and therefore the polymerization process. All tested CTAs were able to reduce shrinkage stress and led to materials with lowered glass transitions and improved impact strength. The ester **ASEE** generally gave the best results, explained principally by its structural similarity to the methacrylate monomers. As a result, the CTA was incorporated rather statistically leading to well-regulated networks. The addition of **ASEE** to the dimethacrylate resin provided polymers with lower and sharper glass transition temperatures with impact strength 2.5 times that of the control.

TABLE 5 Results of the Dynstat Impact Resistance Tests with Commercial Monomers UDMA and D_3MA in Equimolar Ratio and Various CTAs

Network	CTA	[CTA] (db%)	Impact Resistance (kJ mm^{-2})
A	–	0	4 ± 1
B	**ASEE**	5	10 ± 1
C	**ASEE**	20	11 ± 1
D	**ASA**	5	6 ± 1
E	**ASA**	20	7 ± 2
F	**ASN**	5	5 ± 1
G	**BAS**	5	9 ± 3

ACKNOWLEDGMENT

Financial support from Ivoclar Vivadent AG and the Christian Doppler Research Association is gratefully acknowledged. The authors thank Georg Gescheidt and TU Graz/NAWI Graz for the use of the LFP equipment.

REFERENCES AND NOTES

1 B. Husár, S. C. Ligon, H. Wutzel, H. Hoffmann, R. Liska, *Prog. Org. Coat.* **2014**, *77*, 1789–1798.
2 N. Moszner, U. Salz, *Prog. Polym. Sci.* **2001**, *26*, 535–576.
3 Fleischer, J. E. *Mod. Paint Coat.* **2001**, *91*, 21–22, 25.

4 S. Baudis, F. Nehl, S. C. Ligon, A. Nigisch, H. Bergmeister, D. Bernhard, J. Stampfl, R. Liska, *Biomed. Mater. (Bristol, U. K.).* **2011**, *6*, 055003 (12pp).

5 J. Stampfl, S. Baudis, C. Heller, R. Liska, A. Neumeister, R. Kling, A. Ostendorf, M. Spitzbart, *J Micromech. Microeng.* **2008**, *18*, 125014

6 H. Lu, J. W. Stansbury, C. N. Bowman, *Dent. Mater.* **2004**, *20*, 979–986.

7 N. Moszner, *Macromol. Symp.* **2004**, *217*, 63–75.

8 F. Sanda, T. Endo, *J. Polym. Sci. Part A: Polym. Chem.* **2000**, *39*, 265–276.

9 W. D. Emmons, A. W. Gross, (Rohm & Haas Company) Patent US 5399642, **1993**.

10 C. E. Hoyle, C. N. Bowman, *Angew. Chem. Int. Ed.* **2010**, *49*, 1540–1573.

11 C. E. Hoyle, T. Y. Lee, T. Roper, *J Polym. Sci. Part A: Polym. Chem.* **2004**, *42*, 5301–5338.

12 A. Mautner, X. Qin, H. Wutzel, S. C. Ligon, B. Kapeller, D. Moser, G. Russmueller, J. Stampfl, R. Liska, *J. Polym. Sci. Part A: Polym. Chem.* **2013**, *51*, 203–212.

13 P. Esfandiari, S. C. Ligon, J. J. Lagref, R. Frantz, Z. Cherkaoui, R. Liska, *J. Polym. Sci. Part A: Polym. Chem.* **2013**, *51*, 4261–4266.

14 D. Colombani, P. Chaumont, *Prog. Polym. Sci.* **1996**, *21*, 439–503.

15 G. Moad, E. Rizzardo, S. H. Thang, *Acc. Chem. Res.* **2008**, *41*, 1133–1142.

16 G. Moad, E. Rizzardo, S. H. Thang, *Polymer* **2008**, *49*, 1079–1131.

17 D. Zhuo, Y. Ruan, X. Zhao, R. Ran, *J. Appl. Polym. Sci.* **2011**, *121*, 660–665.

18 S. Yamago, Y. Nakamura, *Polymer* **2013**, *54*, 981–994.

19 W. K. Busfield, C. I. Zayas-Holdsworth, S. H. Thang, *J. Polym. Sci. Part A: Polym. Chem.* **2001**, *39*, 2911–2919.

20 H. Lu, J. A. Carioscia, J. W. Stansbury, C. N. Bowman, *Dent. Mater.* **2005**, *21*, 1129–1136.

21 C. Gorsche, M. Griesser, G. Gescheidt, N. Moszner, R. Liska, *Macromolecules* **2014**, *47*, 7327–7336.

22 C. Gorsche, T. Koch, N. Moszner, R. Liska, *Polym. Chem.* **2015**, *6*, 2038–2047.

23 S. C. Ligon, K. Seidler, C. Gorsche, M. Griesser, N. Moszner, R. Liska, *J. Polym. Sci. Part A: Polym. Chem.* **2015**, early view, doi: 10.1002/pola.27788.

24 B. Ganster, U. K. Fischer, N. Moszner, R. Liska, *Macromolecules* **2008**, *41*, 2394–2400.

25 C. Dworak, S. Kopeinig, H. Hoffmann, R. Liska, *J. Polym. Sci. Part A: Polym. Chem.* **2009**, *47*, 392–403.

26 I. W. Harvey, E. D. Phillips, G. H. Whitham, *Tetrahedron* **1997**, *53*, 6493–6508.

27 D. Colombani, C. Navarro, M. Degueil-Castaing, B. Maillard, *Synth. Commun.* **1991**, *21*, 1481–1487.

28 X. Q. Li, X. S. Xu, C. Zhou, *Chem. Commun.* **2012**, *48*, 12240–12242.

29 A. A. Pudikova, N. P. Gerasimova, Y. A. Moskvichev, E. M. Alov, A. S. Danilova, O. S. Kozlova, *Russ. J. Org. Chem.* **2010**, *46*, 352–354.

30 T. Otsu, M. Inoue, B. Yamada, T. Mori, *J. Polym. Sci. Part C: Polym. Lett.* **1975**, *13*, 505–510.

31 J. Brandrup, E. H. Immergut, E. A. Grulke, Polymer Handbook, 4th ed.; Wiley: New York, **2004**.

32 X. Xie, T. E. Hogen-Esch, *Macromolecules* **1996**, *29*, 1746–1752.